Antarctic Science 27(2), 173–184 (2015) © Antarctic Science Ltd 2014 doi:10.1017/S0954102014000558

Sediment transport dynamics on an ice-covered lake: the 'floating' boulders of Lake Hoare, Antarctica

PHILLIP P. ALLEN[1], RICHARD HEWITT[2], MACIEJ K. OBRYK[3] and PETER T. DORAN[3]

[1]Department of Geography, Frostburg State University, Frostburg, MD 21532-2303, USA
[2]Department of Geography, University of Alcalá, Calle Colegios 2, 28801 Alcalá de Henares, Madrid, Spain
[3]Department of Earth & Environmental Sciences, University of Illinois at Chicago, Chicago, IL 60607, USA
ppallen@frostburg.edu

Abstract: Between 1995 and 2011 a global positioning system survey of 13 boulders and three ablation stakes (long stakes frozen in the ice) on the frozen surface of Lake Hoare was undertaken. Data interpretation illustrates complexities of post-depositional transport dynamics of boulders. Earlier studies on comparable datasets have suggested linear 'conveyor' type transport mechanisms for lake surface boulders. Yet explanations for non-linear boulder displacements or 'walks' and the mechanisms responsible for movements are inadequate. Two modes of boulder specific movement were observed. First, localized changes in the ice surface promote individual boulder movement (rolling). Second, ice rafting, which indicates the displacement of 'plates' of lake ice on which the boulder is located. Ablation stakes used as fixed survey control points support the hypothesis that ice cover moves as discrete plates rather than as a single homogenous mass. Factors that create the conditions to generate either of the two modes of movement may be related to location specific energy budgets. A relationship between average orientations and prevailing wind direction was also observed. The investigation describes the local-scale behaviour of surveyed boulders, and offers methodologies and interpretive frameworks for additional studies of modern and ancient sediment transportation dynamics in Antarctic lacustrine environments.

Received 31 October 2013, accepted 16 June 2014, first published online 23 September 2014

Key words: lake ice, non-linear, plate, rafting, rolling

Introduction

The McMurdo Dry Valleys (MDVs) of southern Victoria Land is the largest ice-free region in Antarctica due to the combination of low precipitation and the Transantarctic Mountains that block the down-valley flow of ice from the Polar Plateau (Doran *et al.* 1994). One of the more notable features of the MDVs is the presence of perennially ice-covered lakes. Ice loss from the surface cover of the lakes is principally via sublimation during the winter, and a combination of sublimation, melt and evaporation during the summer (Dugan *et al.* 2013). Mass loss is roughly balanced by new ice formation at the bottom of the ice when the ice covers are in steady state (McKay *et al.* 1985).

The ice covers of the MDVs lakes contain variable amounts of sediment that appears to play a large role in ice surface morphology (Squyres *et al.* 1991). Many of the lakes exhibit a diverse range of sedimentary deposits which, for the purpose of this paper, are defined as poorly sorted and unconsolidated material of variable size. The boulders on the ice-covered surface of the lakes have received attention in previous investigations (e.g. Squyres *et al.* 1991, Chinn 1993), yet our understanding of their origin and movement remains rudimentary. Several hypotheses have been proposed to account for the transport mechanisms that lead to the presence of the 'floating' boulders. These include: i) a diapiric mechanism whereby the debris is frozen to the bottom of the ice and transported to the surface by vertical ice turnover (Bell 1967, Bradley & Palmer 1967, Hendy *et al.* 1972, Chinn 1993), ii) direct deposition of debris from proglacial contact during the replacement of glacial ice by lake ice (Bell 1967, Pickard & Adamson 1983, Doran *et al.* 2000), iii) mass wasting and rolling from slopes, especially on the north side, where the slope angle is steeper and attains an elevation of 1500 m (Squyres *et al.* 1991, Doran *et al.* 1994). However, on Lake Hoare (LH) it is possible that the boulders may have also been directly deposited from supraglacial material by Canada Glacier, due to their confluence at the north-eastern edge of the lake. Understanding the sediment dynamics on and through frozen lake surfaces is significant as it can provide valuable insight into the evolution of the MDVs lake systems. Understanding sedimentation in these lakes aids our interpretation of modern and ancient Antarctic lacustrine depositional sequences. Wand & Perlt (1999) undertook a geodetic survey of ice-rafted boulders on Lake Untersee, Queen Maud Land, East Antarctica and determined the direction and velocity of their movement, and were able

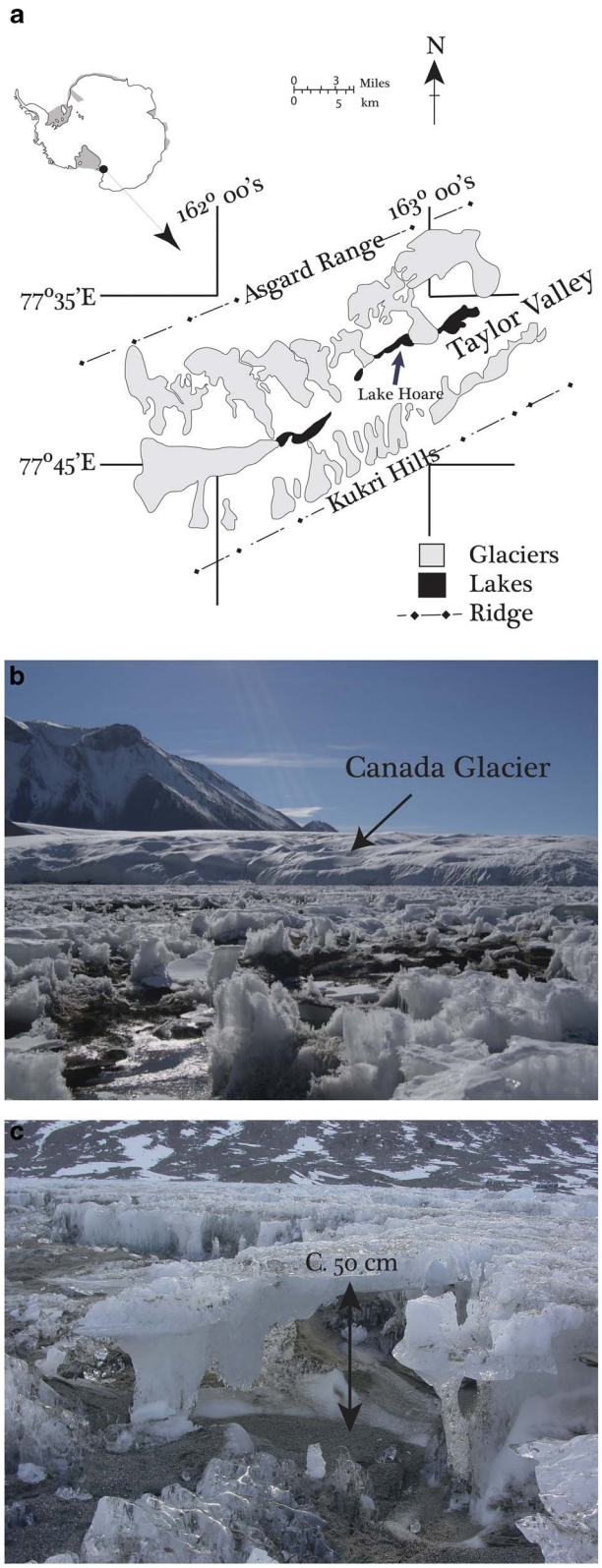

Fig. 1. a. Location of study site. **b.** Irregular surface of Lake Hoare (LH). **c.** Ice pedestal and aeolian sediment deposits on the surface of LH.

to estimate residence time of the boulders on the lake. The focus of this paper is to analyse the results of a 16-year monitoring programme with the aim of characterizing the observed patterns of boulder movement on the surface of ice-covered LH, Taylor Valley (Fig. 1a). The paper explores how boulders on the surface of LH behave, and explains the dynamics of their behaviour across the lake surface.

Site description

Lake Hoare is covered with perennial ice with a thickness in excess of 3 m (Doran *et al.* 2002a). The mean annual air temperature at LH was -17.7°C between 1985 and 2000; however, temperatures frequently rise above 0°C during the summer (Doran *et al.* 2002b). Winters are characterized by strong westerly winds descending from the Polar Plateau, while summer winds are lighter and predominantly from the east (Doran *et al.* 2002b). Lake Hoare is 4.1 km in length and *c.* 1 km at its widest point with a surface area of 1.8 km^2 (Nedell *et al.* 1987, Squyres *et al.* 1991). The lake is dammed by Canada Glacier to the east, which separates LH from Lake Fryxell. To the west is Lake Chad, which has now merged with LH due to lake level rise. The lake receives water from direct glacial melt and from numerous ephemeral streams during the summer months. It is a closed basin, and loses water only by sublimation of ice and evaporation of meltwater. Evaporative loss is enhanced during the 4–12-week summer melt (Welch *et al.* 2010) by the development of open water along the perimeter of the lake, referred to as a 'moat'. The shoreline is composed of poorly consolidated sediment, with boulders up to 0.5 m in diameter (Nedell *et al.* 1987).

The surface of the lake ice is extremely uneven (Fig. 1b & c) with ridges, hollows and ablation tables producing a non-uniform surface morphology. Visual estimates of total percentage surface sediment cover, based on aerial photos, are between 40–50% (Nedell *et al.* 1987). The irregular surface of LH may assist in the retention of the unevenly distributed sedimentary cover. The origin of fine sediments can be attributed to aeolian transport and meltwater discharge, onto the ice (Andersen *et al.* 1993). However, aeolian and fluvial transportation mechanisms cannot explain the presence of the boulders on the ice surface. Processes of sedimentation through perennial ice covers have been suggested (e.g. Nedell *et al.* 1987, Squyres *et al.* 1991, Andersen *et al.* 1993) via mobility through openings in the ice, but these pathways cannot account for the apparent sorting observed on LH. Models for clast sorting indicate a complex relationship between solar radiation and air temperature with larger clasts (> 5 cm) being frequently found on the ice surface. Fine sand to gravel sized (0.02–5 cm) particles are found

https://doi.org/10.1017/S0954102014000558 Published online by Cambridge University Press

Fig. 2. a. Typical set up of GPS on a boulder (floating boulder 13A in this case). **b.** Close-up of benchmark picture in a. **c.** Typical set up of GPS on an ablation stake (AbS2 in this case).

within the floating ice cover, and clasts of *c*. 5 cm have the ability to melt into the ice faster than it ablates (Hendy 2000). The models of clast sorting do not adequately explain the ranges of clasts sizes found on the surface of LH especially boulders > 1 m in size.

Methods

Field survey

The global positioning system (GPS) survey of LH boulders began in 1995. Sediment grain size categories fall under the classification criteria of Lewis (1984) which defines clay as < 3.9 μm, silt 3.9–62.5 μm, sand 62.5 μm–2 mm, gravel (including granule, pebble and cobble) 2–256 mm, and boulders > 256 mm.

The positions of five boulders were initially recorded (Fig. 2a) in 1995, with additional boulders and three ablation stakes being added into the survey during subsequent years, resulting in a total of 13 boulders and three ablation stakes positions being regularly recorded. The surveys were undertaken using Trimble 4000, 4700, 5700's and R7's dual-frequency GPS receivers. Receivers were set to rapid static mode using Trimble Compact L1/L2 and Trimble Zephyr Geodetic antennas located directly above installed survey benchmarks (Fig. 2b). Observation times were between 10–20 minutes at each benchmark. Ablation stakes are segmented transparent acrylic tubes with cross pieces of acrylic mounted at regular intervals to prevent vertical slippage in the ice (Fig. 2c). During the survey, ablation stakes needed to be reinstalled relatively close to their original location. The commencement and survey frequency of boulders and ablation stakes varied but position measurements were recorded using rectangular Universal Transverse Mercator (UTM) co-ordinates.

Surveyed boulders were given an identification number and had a benchmark established on them with a rock drill and expansion bolt. Additionally, three boulders had benchmarks established at each end of their long-axis in order to ascertain rotational movement.

Vector statistics

The UTM data were converted to polar co-ordinates giving yearly movement or 'walk' magnitude (in metres) and walk direction bearings in geographical decimal degrees (i.e. 0 indicating north, clockwise angle rotation). Using the initial boulder survey location as the starting point, the year-to-year displacement of each boulder was examined by investigating the individual movement vectors and then calculating the sum vectors. The method applied, the resultant vector method, is a well-known statistical technique for calculating average directions (Fisher 1995). The average vector, the resultant (R), is a complex number with two components M and Θ.

Annual movements of the boulders and ablation stakes (n) were expressed as vectors having magnitude m and direction θ. These vectors were expressed in component

https://doi.org/10.1017/S0954102014000558 Published online by Cambridge University Press

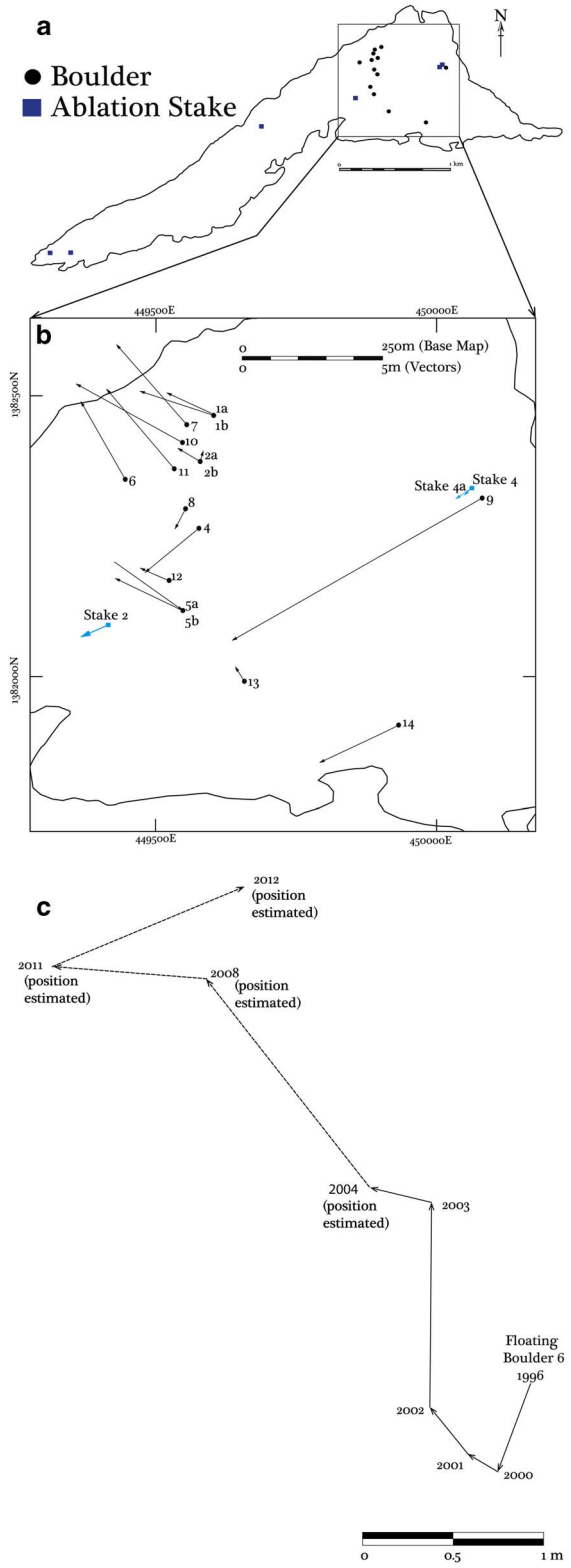

Fig. 3. a. Initial boulder and ablation stake positions. **b.** Total individual annual boulder and ablation stake vectors. **c.** Individual annual vector plots of floating boulder 6 1996–2012.

form (i,j). All i and all j for each vector were summed to produce I and J as shown in:

$$I = \sum_{x=1}^{n} m(\cos\theta_x) \tag{1}$$

$$J = \sum_{x=1}^{n} m(\sin\theta_x). \tag{2}$$

Resultant vector direction Θ can be found by:

$$\Theta = \operatorname{atan}\left(\frac{J}{I}\right). \tag{3}$$

Resultant vector magnitude M is found by:

$$|M| = \sqrt{\left(\sum i_x\right)^2 + \left(\sum j_x\right)^2}, \tag{4}$$

Which is equivalent to:

$$|M| = \sqrt{I^2 + J^2} \tag{5}$$

Boulder/ablation stake dynamics were analysed by calculating the circular variance, s, corresponding to the degree of lateral movement of each boulder/ablation stake throughout the survey period. To calculate s, a similar procedure is followed as in Eqs (1)–(5), except that it is necessary to treat all vectors as unit vectors (magnitude of 1) rather than using real magnitudes. Therefore, I and J are recalculated assuming $m = 1$ for all vectors, this gives a different resultant term, r, calculated as follows:

$$r = \frac{\sqrt{I'^2 + J'^2}}{n}. \tag{6}$$

Circular variance, the inverse of r, is found by:

$$s = 1 - r. \tag{7}$$

The total distance (T) walked over the survey period by each boulder/ablation stake was found simply by the arithmetical sum of all the walk distances (w):

$$T = \sum_{x=1}^{n} w_x, \tag{8}$$

where each walk distance (w_x) is an annual walk for each surveyed boulder equivalent to m (Eqs 1 & 2).

Walk deviations were calculated by taking the difference between resultant vector magnitude (M) and total walk distance (T). The larger the difference, the greater the walk deviation from the average direction of the boulder's journey over the course of survey campaign. The correlation between s scores and walk deviations was investigated by calculating Pearson's correlation coefficient (r) using R software.

The walk deviation ratios were calculated by dividing the resultant vector magnitude by the number of vectors, producing the vector resultant mean. The vector resultant mean is then compared to the vector total mean, the

https://doi.org/10.1017/S0954102014000558 Published online by Cambridge University Press

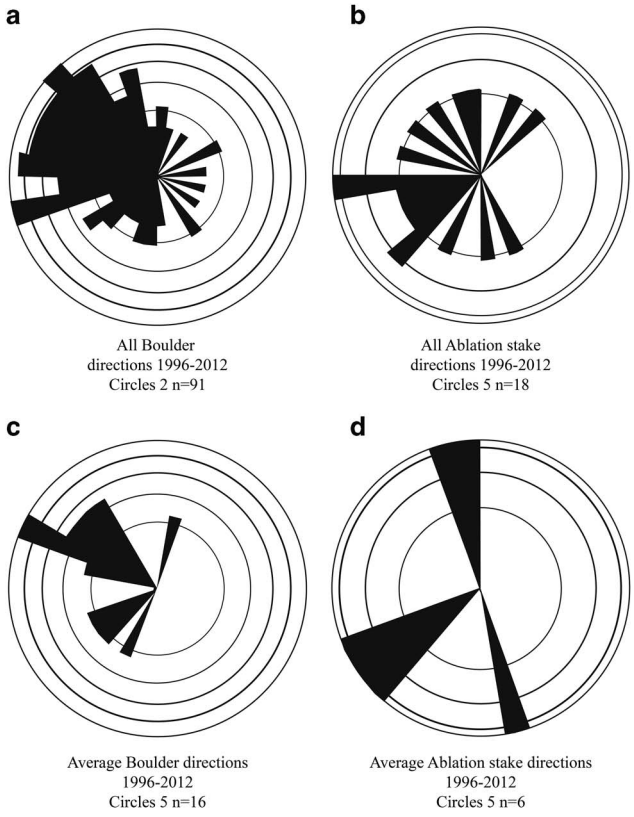

Fig. 4. Rose diagram plots of: **a.** all boulder vectors 1996–2012, **b.** all ablation stake vectors 1996–2012, **c.** resultant boulder vectors 1996–2012, **d.** average ablation stake vectors 1996–2012.

higher the difference between the values the greater the boulder/stake deviates from a single orientation.

Annual wind directions were found using the standard vector sum methodology: Mardia's method (Mardia & Jupp 1999) (Eqs 1, 2 & 3), assuming the unit vector ($m = 1$). The software R was used to plot orientation data for boulders and ablation stakes (Hornik 2010). Wind vectors in the form of square root scaled rose diagrams (e.g. Fisher 1995, Wells 2000) were plotted using GEOrient software (Holcombe 2013). Two statistical tests were carried out: i) the Rayleigh test (see Fisher 1995, Bernatchez 2010), frequently used where a single preferential orientation trend is expected, and ii) Kuiper's test (Bogdan *et al.* 2002), which is more appropriate in cases where more than one preferential orientation is suspected in the dataset.

Results

The boulders selected for this study are broadly distributed across the north-east/north central area of LH, up to *c.* 1 km west of Canada Glacier (Fig. 3a). Resultant vectors showing the displacement of each boulder over the entire survey period are plotted in Fig. 3b. Generally, the boulders appear to be migrating in two dominant directions: south-west and north-west, but individual year-to-year movement is not always in a consistent direction (Fig. 3c).

Rose diagram plots (Fig. 4) of all boulder vector directions show that individual boulder movement trend predominantly south-west, west or north-west (Fig. 4a). However, average boulder vector directions over the whole of the survey window, given by the resultant vectors (Fig. 4c), indicate a predominantly north-westward trend. All ablation stakes vectors appear to have a stronger trend to west and south-west (Fig. 4b & d). In both statistical tests (Table I), the null hypothesis (uniform orientation; no orientation preference) was rejected for all of the boulder data groups (vector dataset 1, 2, 5 and 6 in Table 1) at $P < 0.01$. The null hypothesis could not be rejected at the comparable p-value for the ablation stakes (vector datasets 3, 4, 7, 8 in Table I), either because of the small size of the ablation stake datasets or because the ablation stakes, as would be expected, do not behave in the same way as the boulders.

Vector walk deviation of the boulders and ablation stakes are presented in Table II. Low values indicate very little deviation from a uniform orientation, whereas higher values represent varied directions of movement. The ablation stakes show relatively little walk deviation,

Table I. Significance values of statistical tests applied to all vector datasets.

Dataset	Vector dataset	No. vectors	Test	Test statistic	Significance (P)
1	All boulders 1996–2012	91	Rayleigh	0.62	< 0.01
2	All boulders 1996–2012	91	Kuiper	4.60	< 0.01
3	All ablation stakes 1996–2012	18	Rayleigh	0.47	0.01
4	All ablation stakes 1996–2012	18	Kuiper	1.61	< 0.15
5	All boulders 1996–2004	66	Rayleigh	0.66	< 0.01
6	All boulders 1996–2004	66	Kuiper	4.01	< 0.01
7	All ablation stakes 1996–2004	8	Rayleigh	0.64	0.03
8	All ablation stakes 1996–2004	8	Kuiper	1.85	< 0.05

https://doi.org/10.1017/S0954102014000558 Published online by Cambridge University Press

Table II. Individual measurements of vector deviation for boulders and ablation stakes (T is in metres).

Boulder/stake	*n*	Vector total (T)	Vector resultant mean (M/*n*)	Vector total mean (T/*n*)	Vector walk deviation
FB1A	5	1.95	0.37	0.39	0.02
FB1B	5	2.88	0.55	0.58	0.03
FB2A	5	1.45	0.07	0.29	0.21
FB2B	5	2.55	0.18	0.51	0.33
FB4A	7	6.16	0.36	0.88	0.52
FB5A	6	3.77	0.50	0.63	0.13
FB5B	5	4.00	0.54	0.80	0.26
FB6	8	6.02	0.40	0.75	0.35
FB7	7	4.62	0.55	0.66	0.11
FB8	7	5.51	0.12	0.79	0.67
FB9	7	12.54	1.48	1.79	0.32
FB10	5	5.10	0.86	1.02	0.16
FB11	6	4.27	0.62	0.71	0.09
FB12	5	2.94	0.56	0.59	0.03
FB13	2	0.62	0.31	0.31	0.00
FB14	6	9.04	1.30	1.51	0.21
AbS2 centre	7	1.24	0.15	0.18	0.02
AbS2 A	1	1.76	1.76	1.76	0.00
AbS3 west	7	1.04	0.10	0.15	0.05
AbS3 A	1	1.67	1.67	1.67	0.00
AbS4 east	1	0.68	0.68	0.68	0.00
AbS4 At	1	0.77	0.77	0.77	0.00

as do floating boulders FB1, FB12 and FB13, while some of the boulders (FB4A, FB8) deviate considerably (Table II).

Results of circular variance (*s*) between the individual vectors of a given boulder or stake are summarized in Table III. Low values indicate very little circular variance, i.e. the boulder moved consistently in a single direction. High values indicate more widely varying circular movement, i.e. the boulder repeatedly changed direction. The correlation between *s* and walk deviation was $r = 0.527$ ($P = 0.01$, $n = 22$), suggesting that boulders having greater walk deviation are also those whose movement varied the most about the circle. Ablation stakes showed very little walk deviation with respect to

Table III. Individual movement data and circular variance of boulders and ablation stakes, where high *s* values equate to more variation of circular movement, i.e. the boulder records non-linear movements (T and M are in metres).

Boulder/stake	*n*	Direction (Θ)	Magnitude (M)	Total walk distance (T)	Walk deviation (T-M)	Circular variance (*s*)
FB1A	5	294.88	1.83	1.95	0.12	0.10
FB1B	5	287.78	2.75	2.88	0.13	0.09
FB2A	5	20.29	0.37	1.45	1.07	0.64
FB2B	5	300.61	0.91	2.55	1.64	0.45
FB4A	7	229.92	2.5	6.16	3.67	0.36
FB5A	6	305.26	2.99	3.77	0.79	0.51
FB5B	5	295.02	2.71	4	1.29	0.53
FB6	8	330.1	3.19	6.02	2.83	0.44
FB7	7	318.68	3.85	4.62	0.77	0.24
FB8	7	204.67	0.81	5.51	4.7	0.70
FB9	9	240.29	10.33	12.54	2.21	0.14
FB10	5	298.92	4.29	5.1	0.81	0.32
FB11	6	320.05	3.75	4.27	0.52	0.20
FB12	5	292.34	2.8	2.94	0.15	0.09
FB13	2	328.35	0.61	0.62	0.01	0.01
FB14	6	244.75	7.8	9.04	1.24	0.09
AbS2 centre	7	246.82	1.07	1.24	0.16	0.12
AbS2A	1	353.61	1.76	1.76	0	0.00
AbS3 west	7	166.79	0.71	1.04	0.32	0.85
AbS3A	1	349.68	1.67	1.67	0	0.00
AbS4 east	1	236.5	0.68	0.68	0	0.00
AbS4A	1	223.85	0.77	0.77	0	0.00

https://doi.org/10.1017/S0954102014000558 Published online by Cambridge University Press

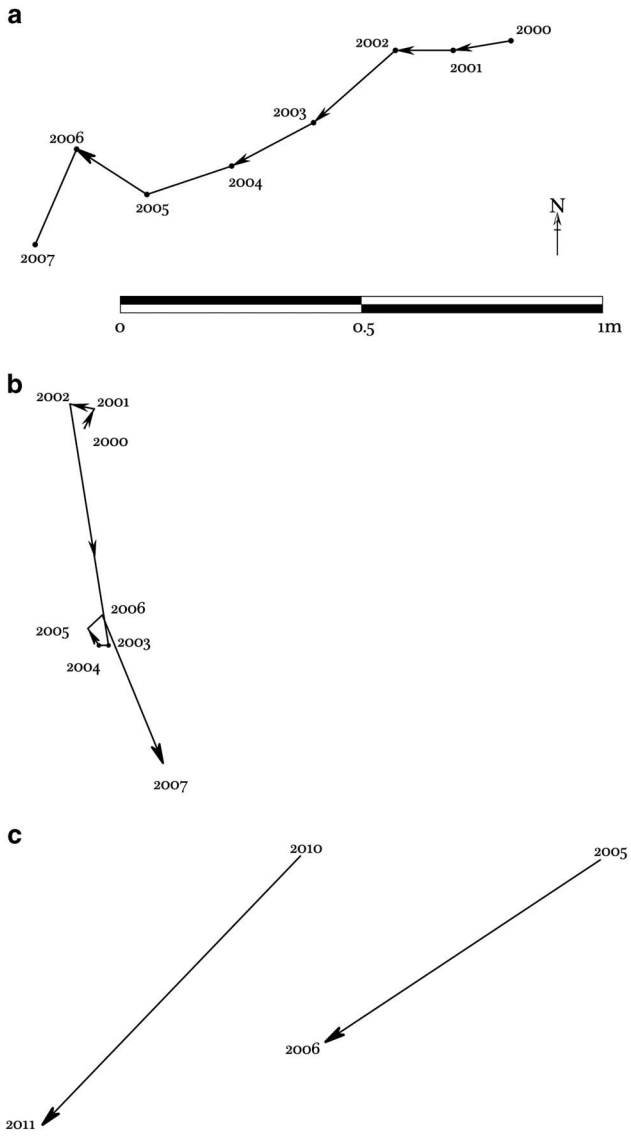

Fig. 5. Individual annual ablation stake vector plots for: **a.** Ablation stake 2 (AbS2) centre 2000–07, **b.** AbS3 west 2000–07, **c.** AbS4 2010–11 and AbS4 east 2005–06 (reinstalled due to loss of original position via ablation).

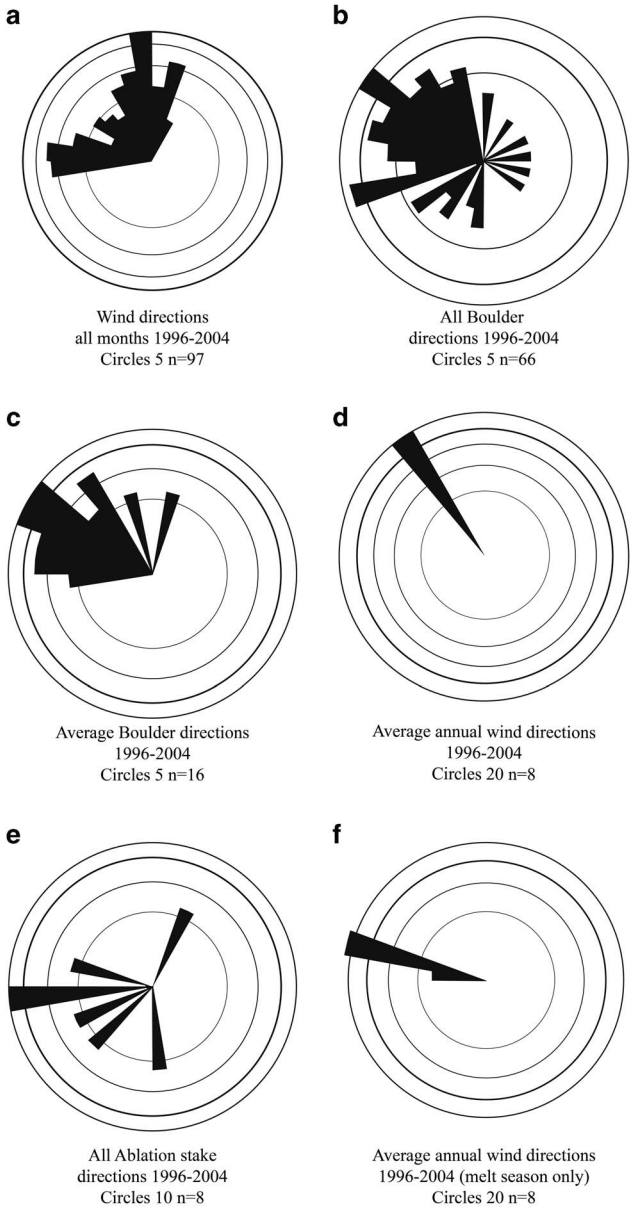

Fig. 6. Comparison of boulder/ablation vectors and wind directions. Rose diagram plots of: **a.** wind directions all months 1996–2004, **b.** all boulders 1996–2004, **c.** average boulder directions 1996–2004, **d.** average annual wind directions 1996–2004, **e.** all ablation stakes directions 1996–2004, **f.** average annual wind direction 1996–2005 November–January (melt season only).

the boulders, with an exception of one outlier, AbS3 west (Table III). The implication is that, while the ablation stakes are clearly moving, the lateral zigzagging 'walk' is unique to the boulders.

The relatively linear movement of individual ablation stakes is clearly seen when the vectors are plotted (Fig. 5a–c). However, since movement data for ablation stakes is limited (only two ablation stakes had more than one vector; see Fig. 5), further monitoring of the existing ablation stakes is required before firm conclusions can be drawn about their pattern of movement.

Square root scaled orientation rose diagrams for wind data, plotted against average boulder directions for the equivalent period clearly illustrate that the average wind direction corresponds to observed boulder movement. Wind data (Fig. 6a) was analysed from 1996–97 to 2003–04 and only boulder orientations (Fig. 6b) up to this date were included in the comparison.

https://doi.org/10.1017/S0954102014000558 Published online by Cambridge University Press

Table IV. Comparison of boulder and ablation stake vectors with wind direction (wind ave).

Boulder/stake	Season				
	1996–2000	2000–01	2001–02	2002–03	2003–04
FB1A	309	332	315	288	255
FB1B	277	324	309	303	256
FB2A	37	259	313	326	121
FB2B	279	344	312	105	298
FB4A	NA	307	276	220	317
FB5A	292	189	310	331	63
FB5B	251	268	343	90	294
FB6	200	301	321	1	284
FB7	286	256	224	346	281
FB8	NA	3	240	184	350
FB9	NA	212	258	293	231
FB10	NA	NA	295	306	281
FB11	NA	NA	284	303	269
FB12	NA	NA	325	305	256
FB13	NA	NA	336	321	NA
FB14	NA	NA	273	255	239
AbS2 centre	NA	261	270	229	242
AbS2A	NA	NA	NA	NA	NA
AbS3 west	NA	27	281	171	270
AbS3A	NA	NA	NA	NA	NA
AbS4 east	NA	NA	NA	NA	NA
AbS4A	NA	NA	NA	NA	NA
All boulders	281.49	290.38	297.16	306.83	277.59
All stakes	-	143.55	275.65	199.74	256.05
Wind ave	-	326.68	323.93	330.41	327.14
Wind ave_melt season	-	285.35	281.63	286.55	280.22

If the data are examined together (Table IV), this strong correlation becomes apparent. For 2000–01, it can be seen that the average walk direction for all boulders of 290° is very close to the average wind direction during the melt season of 285°. Average directions of boulder walks and wind are also similar for 2001–02 (all boulders: 297°, wind ave_melt: 282°) and for 2002–03 (all boulders: 307°, wind ave_melt: 287°). In the final year for which wind data were available, average boulder walk and wind direction during the melt season differ by only 3° (all boulders: 278°, wind ave_melt: 280°).

Discussion

Two distinct signals that represent a complex relationship that produces the observed movement of the boulders are present within the data. The first signal is actual movement of the boulder independent of the ice, i.e. rolling. This rolling is generated by the localized ablation of the ice surface that is encasing or supporting the boulder. Variation of the ice surface can produce a pedestal that degrades and collapses, and can result in a gravity-assisted rolling of the boulder. Movement of boulders due to the rolling process is clearly demonstrated by the high circular variance values for FB2, FB5, FB6 and FB8 (Table III). FB2 has been chosen as a characteristic example of localized rolling. The plots of FB2A/B (Fig. 7a) represent two different reference points on the same boulder; the differences between FB2A/B illustrate the highly localized nature of the rolling, as both records do not describe a uniform pattern. This indicates the boulder is rolling along its A, B or C axial planes without a preferred orientation. This sporadic and irregular movement is supported by the high s values (0.64 and 0.45, respectively) and walk deviation (Table III), which demonstrate that the boulder did not move consistently in a single direction.

The mechanism of ice loss and rejuvenation at LH and other Taylor Valley lakes is well established (Henderson *et al.* 1966, Chinn 1993). The loss of surface ice via ablation has the ability to expose boulders to sunlight, which is absorbed and re-radiated by the rock material, further adding to the differential melting/sublimation of the ice surface. The observed north-west movement of a lot of the boulders may be related to sun tracking. Although this area experiences 24 hours of sunlight in the summer, there is far more solar insolation from the north where the sun rises much higher in the sky than in the south. Therefore, the north side of the boulders and associated surface alluvial sediments get warmed during daylight hours, which creates hollows into which the boulders can tip. This was observed in the field. At LH the high cliff due north of the lake creates a shadow

https://doi.org/10.1017/S0954102014000558 Published online by Cambridge University Press

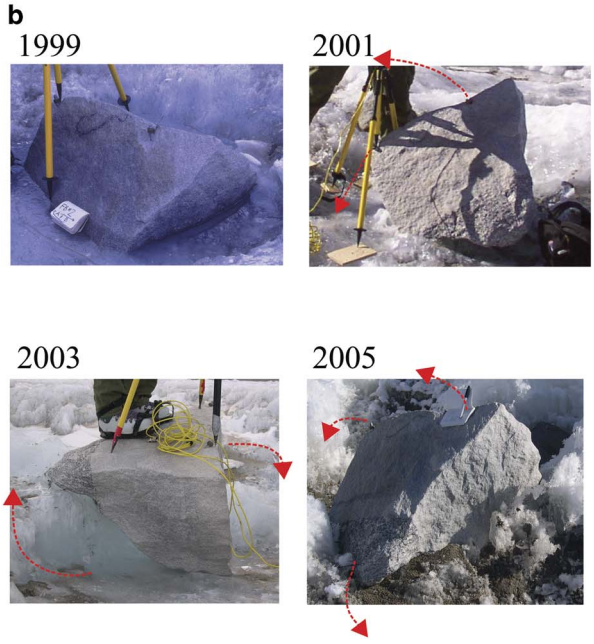

Fig. 7a. Survey positions and vectors of floating boulder 2A (FB2A) (top) and FB2B (bottom) attributed to boulder rolling. **b.** Orientation changes of FB2 during 1999, 2001, 2003 and 2005 (dashed lines with arrows indicate coarse changes in position from previous photo).

around solar noon, which makes for a deflection away from due north.

Non-uniform loss of ice can also result in ice pedestal formation (Hendy 2000) and continued melt can undercut the boulder and creates a void in to which the boulder eventually falls and promotes the rolling movement. The process of boulder uplift and rolling has been recorded,

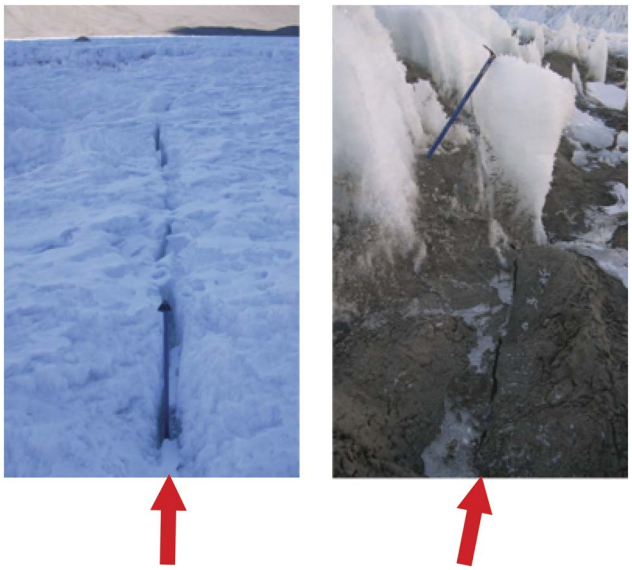

Fig. 8. Extensive cracks of ice surface indicating possible ice plate boundaries.

at a fairly coarse resolution, in a series of photographs (Fig. 7b) covering the 1999, 2001, 2003 and 2005 summers. In 1999, FB2A/B is encased in ice, yet by 2001 the surface ice has been lost and the boulder attained some degree of movement. The photograph from 2003 demonstrates the ice pedestal supporting the boulder. Between 2003 and 2005 ablation of the ice pedestal occurs and results in boulder movement. Thus, a relatively minor movement of the boulder can be enhanced by the uneven surface. This enhancement probably accounts for the pronounced shifts seen in the plotted data (Fig. 7a). The accumulation of aeolian deposits in close proximity to the boulder (Fig. 7b 2005) may further assist in the ice reduction as this is known to be an efficient heat transmitter in this environment, promoting localized melting (Squyres *et al.* 1991).

The second signal apparent in the data represents movement in an almost uniform orientation. These boulders are not demonstrating independent and individual movement along their A, B or C axial planes, but their walks reflect the movement of the ice on which the boulders are located. Vertically extensive cracks (Fig. 8) through the ice cover are frequently observed and are a known pathway for sediment to enter the lake environment (Nedell *et al.* 1987, Squyres *et al.* 1991). These cracks may represent the limits of multiple individual plates across LH, which can move as independent discrete blocks of ice.

This movement is demonstrated by FB1 (Fig. 9a) where the boulder rests on a plate of ice much like an object on a raft, and its walk is describing the movements of the underlying ice. The control for this rafting movement is probably the wind as there is a strong correlation between

https://doi.org/10.1017/S0954102014000558 Published online by Cambridge University Press

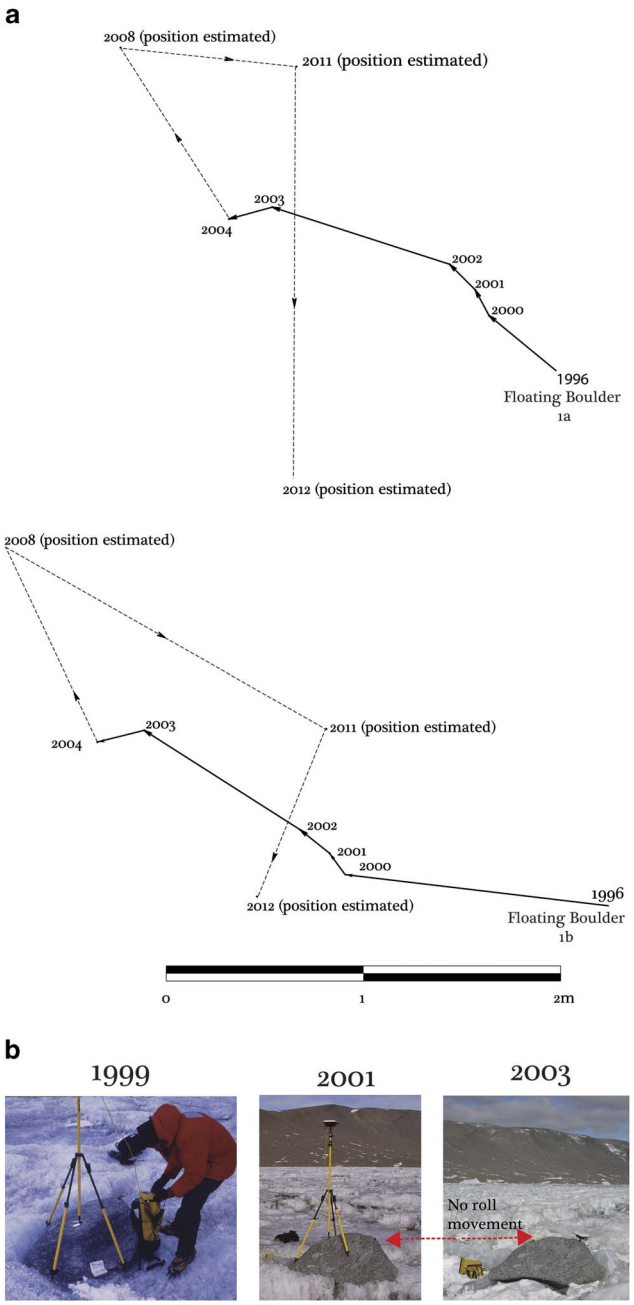

Fig. 9a. Survey positions and vectors of floating boulder 1 (FB1A and FB1B) attributed to ice rafting. **b.** Orientation changes of FB1 during 1999, 2001 and 2003.

the mean annual wind vectors and the boulder movement (Fig. 6d and Table IV). The plots of FB1A/B represent two different reference points on the same boulder (Fig. 9). However as with FB2A/B there is a difference between the plotted walks of the two points, this represents minimal independent movement of the boulder over time. The two plots of FB1A/B do not describe an identical pattern but the overall trend is exceptionally similar, which indicates that the boulder is not significantly rolling along its A, B and C axial planes but actually retains a preferred or almost static orientation. The lack of movement is illustrated in a series of photos from 1999, 2001 and 2003 (Fig. 9b). These images show almost no movement of the boulder yet the ice surface remains active over the same period. The interpretation of severely reduced lateral movements of boulder FB1A/B is supported by the low walk deviation and *s* values (0.02, 0.10 and 0.03, 0.09 and Table II and III, respectively) demonstrating boulder movement in a consistent almost uniform direction. Due to the undulating topography of the ice surface on LH, the simplest explanation for this movement is that the boulder remained in a preferred position and that the ice was moved by the prevailing winds. During the summer a pronounced moat frequently develops around the lake margins. The moat allows movement to be achieved by the surface ice, and once the moat refreezes the new position of the boulder is achieved.

The ablation data from stakes AbS2 and AbS3 demonstrates that the ice movement is not uniform, nor is it moving as one homogenous surface (Fig. 5a–c; only ablation stakes AbS2, AbS3 and AbS4 are shown, as ablation stake AbS1 disappeared soon after the survey started). The three ablation stakes exhibited contrasting movements. Therefore, during the summer, the surface of LH is not moving as a single mass, but rather as a number of discrete plates. This seems to be consistent with the observations made earlier with respect to the ablation stakes, particularly AbS3 which showed very high circular variance, but low walk deviation. Plots of the ablation stakes generally illustrate very little walk deviation even where circular variance was high. Therefore, ablation stakes do move, but do not appear to show the displacement that is characteristic of the boulders.

Boulder size is not considered an instrumental factor in determining the style of movement, as boulders with varied and comparable sizes were recorded exhibiting both mechanisms of movement. For example, the A, B and C axis of FB6 is 1.8, 1.42 and 0.43 m, respectively, and it rolls, while the A, B and C axis of FB11 was 1.91, 1.79 and 0.5 m, respectively, and it moves via rafting. Variation in ice development and loss may be related to the distribution of fine grain sediment that is efficient in energy absorption. The movement of boulders due to rolling is clearly demonstrated, yet the size of individual boulders does not appear to exert any significant influence. An exact causal factor that is responsible for individual movement is difficult to identify. Boulders that have been moved by rafting also display no relationship between mode of movement and size. The recorded movements of all the surveyed boulders during the 16-year study do not describe a linear 'conveyor' type pattern at the scale of the individual annual walk, as observed by Wand & Perlt (1999). However, this kind of linear 'conveyor' pattern does become apparent when

https://doi.org/10.1017/S0954102014000558 Published online by Cambridge University Press

vectors representing overall start and finish positions are plotted. The main differences between the results of this study and those of Wand & Perlt (1999) are rolling and rafting movements of the LH boulders. One other clear difference is the lack of realistic reference points for the origin of the LH boulders on the ice. Unlike Wand & Perlt (1999), the boulders of LH are not associated with a specific known point of origin. Thus the movement away from the point of origin cannot be accounted for and, therefore, our data is inconsistent with the conveyor modes of transport. In addition, due to the lack of a fixed reference point for origin on the ice, an accurate residence time for the boulders of LH cannot realistically be calculated. When the start and end points of the survey period are plotted a generalized pattern of movement is displayed, yet this masks the fragmented ice surface movement (rafting), which accounts for some of the boulder movement.

Conclusions

Understanding the sediment dynamics on and through frozen lake surfaces is complex, yet it can provide a significant contribution into the behaviour and evolution of the MDVs lake system. The data generated during the GPS survey campaign illustrate the complexity of boulder movement across the surface of LH and describe two distinct modes of boulder mobility. First, boulder specific movement via localized changes in the ice surface that promotes individual boulder movement (rolling). Second, motion via ice rafting, where the individual boulder demonstrates no significant localized axial plane motion but lake ice on which the boulder sits moves laterally. The factors that create the conditions to generate either of the two modes of movement may be related to available energy. The exposure to 24-hour sunlight across LH during the summer promotes localized ice melt due to differential heating, leading to boulder rolling. Individual ice-rafted boulder movements suggest a fragmented ice surface of LH. The extensive network of cracks observed on the surface may account for the individual movements recorded during the survey period. The data from the ablation stakes support the hypothesis that the ice cover of LH is not moving as one homogenous plate. During the summer, these plates could be moved via shearing due to the action of the wind.

Acknowledgements

We acknowledge the support provided by the National Foundation of Science, Office of Polar Programs to the McMurdo Dry Valleys Long Term Ecological Research (LTER) programme (grant number 1115245). Many thanks to Bjorn Johns, Beth Bartel and Thomas Nylen the UNAVCO field personnel who accurately surveyed the boulders. Additional fieldwork was performed from LTER scientists, Jennifer Knoepfle (nee Lawson), Carrie Olsen and Roman Borochin. We are grateful to Dr Jason Jordan, Dr Jennifer Knoepfle, Dr Marc Michael and Mr Simon Parfitt for comments on an early version of this manuscript, and to the anonymous reviewers.

Author contribution

Phillip P. Allen: undertook field survey for acquisition of data, undertook analysis and interpretation of data, led drafting the manuscript, co-ordinated and incorporated all edits/contributions from other authors, designed and drew graphics and incorporated graphics generated by other authors into final figures, undertook critical revision of manuscript, corresponded with editorial office. Richard Hewitt: led in generation, analysis and interpretation of statistical data, significantly contributed to the drafting of the manuscript, designed and drew graphics relating to vectors plots and rose diagrams, undertook critical revision of manuscript. Maciej K. Obryk: led in providing original raw data in usable format, undertook field surveys for acquisition of data, critical revision of analysis and interpretation of data, contributed to the drafting of the manuscript, undertook critical revision of manuscript. Peter T. Doran: led in study conception and design, led in starting study in the field, undertook field surveys for acquisition of data, critical revision of analysis and interpretation of data, significantly contributed to the drafting of the manuscript, undertook critical revision of manuscript.

References

Andersen, D.W., Wharton, R.A. & Squyres, S.W. 1993. Terrigenous clastic sedimentation in Antarctic Dry Valley lakes. *Antarctic Research Series*, **59**, 71–81.

Bell, R.A.I. 1967. Lake Miers, south Victoria Land, Antarctica. *New Zealand Journal of Geology and Geophysics*, **10**, 540–556.

Bernatchez, J.A. 2010. Taphonomic implications of orientation of plotted finds from Pinnacle Point 13B (Mossel Bay, Western Cape Province, South Africa). *Journal of Human Evolution*, **59**, 274–288.

Bogdan, M., Bogdan, K. & Futschik, A. 2002. A data driven smooth test for circular uniformity. *Annals of the Institute of Statistical Mathematics*, **54**, 29–44.

Bradley, J. & Palmer, D.F. 1967. Ice-cored moraines and ice diapirs, Lake Miers, Victoria Land, Antarctica. *New Zealand Journal of Geology and Geophysics*, **10**, 599–623.

Chinn, T.J. 1993. Physical hydrology of the Dry Valley lakes. *Antarctic Research Series*, **59**, 1–51.

Doran, P.T., Wharton, R.A. & Lyons, W.B. 1994. Paleolimnology of the McMurdo Dry Valleys, Antarctica. *Journal of Paleolimnology*, **10**, 85–114.

Doran, P.T., Wharton, R.A., Lyons, W.B., Des Marais, D.J. & Andersen, D.T. 2000. Sedimentology and geochemistry of a perennially ice-covered epishelf lake in Bunger Hills Oasis, East Antarctica. *Antarctic Science*, **12**, 131–140.

Doran, P.T., McKay, C.P., Clow, G.D., Dana, G.L., Fountain, A.G., Nylen, T. & Lyons, W.B. 2002b. Valley floor climate observations from the McMurdo Dry Valleys, Antarctica, 1986–2000. *Journal of Geophysical Research - Atmospheres*, **107**, 10.1029/2001JD002045.

Doran, P.T., Priscu, J.C., Lyons, W.B., Walsh, J.E., Fountain, A.G., McKnight, D.M., Moorhead, D.L., Virginia, R.A., Wall, D.H., Clow, G.D., Fritsen, C.H., McKay, C.P. & Parsons, A.N. 2002a. Antarctic climate cooling and terrestrial ecosystem response. *Nature*, **415**, 517–520.

Dugan, H.A., Obryk, M.K. & Doran, P.T. 2013. Lake ice ablation rates from permanently ice covered Antarctic lakes. *Journal of Glaciology*, **59**, 491–498.

Fisher, N.I. 1995. *Statistical analysis of circular data*. Cambridge: Cambridge University Press, 296 pp.

Henderson, R.A., Prebble, W.M., Hoare, R.A., Popplewell, K.B., House, D.A. & Wilson, A.T. 1966. An ablation rate for Lake Fryxell, Victoria Land, Antarctica. *Journal of Glaciology*, **6**, 129–133.

Hendy, C.H, Selby, M.J. & Wilson, A.T. 1972. Deep Lake, Cape Barne, Antarctica. *Limnology and Oceanography*, **17**, 356–362.

Hendy, C.H. 2000. The role of polar lake ice as a filter for glacial lacustrine sediments. *Geografiska Annaler - Physical Geography*, **82A**, 271–274.

Holcombe, R. 2013. Structural geology – mapping/GIS software: GEOrient© v9.x. Available at: http://www.holcombe.net.au/software/rodh_software_georient.htm#conditions.

Hornik, K. 2010. *Frequently asked questions on R*. Version 2.11. Available at: http://horacio9573.no-ip.org/R-doc/R-FAQ.html.

Lewis, D.W. 1984. *Practical sedimentology*. Stroudsburg, PA: Hutchinson: Ross, 229 pp.

Mardia, K.V. & Jupp, P.E. 1999. *Directional statistics*. Chichester: John Wiley, 414 pp.

McKay, C.P., Clow, G.D., Wharton, R.A. & Squyres, S.W. 1985. Thickness of ice on perennially frozen lakes. *Nature*, **313**, 561–562.

Nedell, S.S., Andersen, D.W., Squyres, S.W. & Love, F.G. 1987. Sedimentation in ice-covered Lake Hoare, Antarctica. *Sedimentology*, **34**, 1093–1106.

Pickard, J. & Adamson, D.A. 1983. Perennially frozen lakes at glacier/rock margins, East Antarctica. *In* Oliver, R.L., James, P.R. & Jago, J.B. *eds. Antarctic earth science*. Cambridge: Cambridge University Press, 470–472.

Squyres, S.W., Andersen, D.W., Nedell, S.S. & Wharton, R.A. 1991. Lake Hoare, Antarctica: sedimentation through a thick perennial ice cover. *Sedimentology*, **38**, 363–379.

Wand, U. & Perlt, J. 1999. Glacial boulders 'floating' on the ice cover of Lake Untersee, East Antarctica. *Antarctic Science*, **11**, 256–260.

Welch, K.A., Lyons, W.B., Whisner, C., Gardner, C.B., Gooseff, M.N., McKnight, D.M. & Priscu, J.C. 2010. Spatial variations in the geochemistry of glacial meltwater streams in the Taylor Valley, Antarctica. *Antarctic Science*, **22**, 662–672.

Wells, N.A. 2000. Are there better alternatives to standard rose diagrams? *Journal of Sedimentary Research*, **70**, 37–46.